The Novel Therapeutic Effect of Phosphoinositide 3-Kinase-γ Inhibitor AS605240 in Autoimmune Diabetes

The Novel Therapeutic Effect of Phosphoinositide 3-Kinase-γ Inhibitor AS605240 in Autoimmune Diabetes

Jamil Azzi,[1] Robert F. Moore,[1] Wassim Elyaman,[2] Marwan Mounayar,[1] Najib El Haddad,[1] Sunmi Yang,[1] Mollie Jurewicz,[1] Ayumi Takakura,[3] Alessandra Petrelli,[1] Paolo Fiorina,[1] Thomas Ruckle,[4] and Reza Abdi[1]

Type 1 diabetes (T1D) remains a major health problem worldwide, with a steadily rising incidence yet no cure. Phosphoinositide 3-kinase-γ (PI3Kγ), a member of a family of lipid kinases expressed primarily in leukocytes, has been the subject of substantial research for its role in inflammatory diseases. However, the role of PI3Kγ inhibition in suppressing autoimmune T1D remains to be explored. We tested the role of the PI3Kγ inhibitor AS605240 in preventing and reversing diabetes in NOD mice and assessed the mechanisms by which this inhibition abrogates T1D. Our data indicate that the PI3Kγ pathway is highly activated in T1D. In NOD mice, we found upregulated expression of phosphorylated Akt (PAkt) in splenocytes. Notably, T regulatory cells (Tregs) showed significantly lower expression of PAkt compared with effector T cells. Inhibition of the PI3Kγ pathway by AS605240 efficiently suppressed effector T cells and induced Treg expansion through the cAMP response element-binding pathway. AS605240 effectively prevented and reversed autoimmune diabetes in NOD mice and suppressed T-cell activation and the production of inflammatory cytokines by autoreactive T cells in vitro and in vivo. These studies demonstrate the key role of the PI3Kγ pathway in determining the balance of Tregs and autoreactive cells regulating autoimmune diabetes. ***Diabetes*** **61:1509–1518, 2012**

Phosphoinositide 3-kinases (PI3Ks) are a family of dual-specificity kinases with roles in multiple intracellular signaling pathways (1). The phosphoinositides, which are phosphorylated by PI3Ks at the 3′-OH position of the inositol ring, work as a docking platform for lipid-binding domains of various cellular proteins, such as protein kinase-B (PKB)/Akt. The latter triggers downstream kinase cascades involved in many cellular functions including cell survival and proliferation (2). Although PI3Ks are grouped into three classes, class I is the most studied and the most clinically relevant (1). Class IA includes three catalytic subunits, p110α, p110β, and p110δ, that are activated through tyrosine-kinase signaling (3). Class IB (PI3Kγ) is mainly activated by seven transmembrane G-protein-coupled receptors, which include the chemokine receptors (1,4). PI3Kγ has been shown to regulate T-cell activation in a T-cell receptor-dependent manner (5–7). Whereas expression of the PI3Kα and β-subunits is ubiquitous, PI3Kγ expression is mainly restricted to the hematopoietic system (8), which may limit the toxicity of specific inhibition compared with pan-PI3K inhibition. This has sparked great interest in its role in inflammatory diseases such as chronic obstructive pulmonary disease, pancreatitis, rheumatoid arthritis, and systemic lupus erythematosus (SLE) (8–10). As of yet, no data are available on the role of the PI3Kγ pathway in modulating autoimmune responses in type 1 diabetes (T1D) (11–13). Inhibiting a key signaling enzyme in the activation of T cells such as the PI3Kγ molecule can constitute a novel therapeutic modality for T1D, an autoimmune disease characterized by selective damage to pancreatic β-cells mediated mainly by autoreactive T cells ($CD4^+$ and $CD8^+$) (14,15). In this study, we used AS605240, a PI3Kγ inhibitor (PI3Kγ-i) (Merck-Serono), which has shown promising results in several animal disease models (8,9,16,17). We tested the effect of this PI3Kγ-i in preventing and reversing T1D in NOD mice in order to provide mechanistic data. Our results highlight the role of the PI3Kγ pathway in determining the balance of T regulatory cells (Tregs) and autoreactive cells in the pathogenesis of T1D.

RESEARCH DESIGN AND METHODS

Mice. Female NOD/ShiLtJ, BDC2.5, NOD-*scid*, and C57BL/6 mice were purchased from The Jackson Laboratory (Bar Harbor, ME). Animals were maintained under specific pathogen-free conditions at Harvard Medical School.

Acquisition of PI3Kγ-i. AS605240 was obtained through collaboration with Thomas Ruckle at Merck-Serono. Details of the compounds were reported previously (8,9).

Flow cytometric analysis. Anti-mouse Abs for CD62L, CD44, CD4, CD25, CD8, CD11c, CD11b, B220, Annexin (phycoerythrin), 7AAD (PerCP; BD Biosciences), forkhead box protein 3 (FoxP3; eBioscience), and PAkt (S473) (Cell Signaling Technology) were used for fluorescence-activated cell sorter (FACS) analysis.

Autoreactive T-cell proliferation assay. A total of 5×10^5 BDC2.5 splenocytes and 50 μg/mL BDC2.5-peptide were incubated in vitro in a 96-well round-bottom plate for 48 h. We then pulsed the cultures with 1 μCi of tritiated thymidine [^{3}H] to determine cell proliferation.

Enzyme-linked immunospot assay measuring autoreactive T-cell activity. A total of 5×10^4 irradiated NOD dendritic cells, 1×10^5 $CD4^+$ BDC2.5 T cells, and 100 ng/mL BDC2.5-islet-peptide for in vitro studies and 1×10^6 splenocytes with 100 μg/mL BDC2.5-islet-peptide for ex vivo prevention studies were used to assess IFN-γ as described previously (18). We subtracted the number of spots counted in the negative control (absence of peptide) from the number of spots in the stimulated cultures.

Akt (Thr^{308}) ELISA assay. ELISA assay was performed according to manufacturer's protocol [PhosphoDetect Akt (Thr^{308}); Calbiochem, San Diego, CA].

Luminex assay. A 21-plex cytokine kit (Millipore, St. Charles, MO) and an 8-plex-Multi-Pathway Signaling Kit-Phosphoprotein (Milliplex MAP Kit; Millipore) were used according to the manufacturer's instructions.

Pancreas pathology and immunohistochemistry. Pancreas immunohistology was performed as described by our group previously (19). For the quantification of the $PAkt^+CD3^+$ cells, five high-power field areas of spleen were enumerated for color. Green color represented $PAkt^+$ cells; red color represented $CD3^+$ cells. The number of cells showing double positivity for $PAkt^+$ and $CD3^+$

From the [1]Transplantation Research Center, Renal Division, Brigham and Women's Hospital and Children's Hospital Boston, Harvard Medical School, Boston, Massachusetts; the [2]Center for Neurologic Diseases, Brigham and Women's Hospital, Boston, Massachusetts; the [3]Renal Division, Brigham and Women's Hospital, Harvard Medical School, Boston, Massachusetts; and the [4]Therapeutic Area Neurodegenerative Diseases, Merck Serono S.A., Geneva, Switzerland.

Corresponding author: Reza Abdi, rabdi@rics.bwh.harvard.edu.

Received 31 January 2011 and accepted 7 February 2012.

DOI: 10.2337/db11-0134

This article contains Supplementary Data online at http://diabetes.diabetesjournals.org/lookup/suppl/doi:10.2337/db11-0134/-/DC1.

was counted in each of the areas, and the percentage of positive $CD3^+PAkt^+$ cells to positive $CD3^+$ was calculated. The mean of the percentage of the five areas was calculated.

Insulitis score. Insulitis scoring was performed on hematoxylin and eosin–stained pancreatic sections. A score of 0–4 was assigned based on islet infiltration by a blinded pathologist, as previously described (20). Insulitis scores were graded as follows: grade 0, normal islets; grade 1, mild mononuclear infiltration (<25%) at the periphery; grade 2, 25–50% infiltration; grade 3, >50% infiltration; and grade 4, islets completely infiltrated with no residual parenchyma remaining. At least 30 islets per group were analyzed and pooled from sections obtained from at least four different mice.

Isolation of cells from pancreas. The minced pancreas was washed twice with 10 mL Hanks' balanced salt solution plus 10% fetal calf serum. The tissue was resuspended with 10 mL of Iscove's modified Dulbecco's medium containing 1 mg/mL collagenase (type IV; Sigma Chemical, St. Louis, MO) and incubated in a water bath for 30 min at 37°C with continuous shaking (100 cycles/min). Lymphocytes were isolated by Percoll technique and assessed with FACS analysis.

$CD4^+$ T-cell extraction and $CD25^+$ T-cell depletion. $CD4^+$ cell extraction and $CD25^+$ cell depletion from splenocytes of NOD or BDC2.5 mice were conducted using magnetic microbeads (Miltenyi Biotec, Auburn, CA). As measured by FACS analysis, the isolated cell population had a purity >95%.

Treg generation assay. A total of 2.5×10^5 $CD4^+$ T cells from NOD mice were cultured for 72 h with 1 μg/mL anti-CD3, 1 μg/mL anti-CD28, and 1 ng/mL transforming growth factor-β (TGF-β) with and without AS605240 (5 μM).

Adoptive cell transfer. A total of 20×10^6 whole splenocytes or Treg-depleted splenocytes extracted from hyperglycemic NOD mice or AS605240-treated mice were adoptively transferred into NOD-*scid* hosts. Onset of diabetes was monitored at least three times per week.

Western blot. Western blots were performed as previously described (21).

Statistical analyses. Data are expressed as mean ± standard error. Kaplan-Meier analysis was used for survival analysis, and a log-rank comparison of the groups was used to calculate *P* values. The *t* test was used for comparison of means between the experimental groups. Differences were considered to be significant when *P* was <0.05.

RESULTS

PI3Kγ-i AS605240 suppresses intracellular PAkt in splenocytes of NOD mice. To examine the activity of the PI3K–Akt pathway in autoimmune diabetes, lysates of splenocytes from early diabetic NOD mice were subjected to an ELISA assay that measures the level of Akt protein phosphorylated at Thr^{308}. As shown in Fig. 1*A*, PAkt expression was significantly increased in the splenocytes of NOD mice compared with those from naive C57BL/6 mice of the same age. We then assessed the expression of PAkt in spleens of untreated NOD mice versus NOD mice treated with 30 mg/kg of AS605240 administered i.p. daily for 7 days. Immunohistochemistry of splenocytes using 4',6-diamidino-2-phenylindole, CD3, and intracellular PAkt staining was performed. Histological analysis revealed significant suppression of positive PAkt in splenocytes of treated mice compared with control mice. The percentage of $CD3^+$ cells expressing PAkt was significantly reduced in treated compared with control mice (38.04 ± 11.03% vs. 65.40 ± 6.78%, respectively; $P = 0.002$) (Supplementary Fig. 1). Western blot performed on splenocytes from AS605240-treated and control NOD mice showed suppression of PAkt in the spleen of treated NOD mice compared with control (Fig. 1*B*).

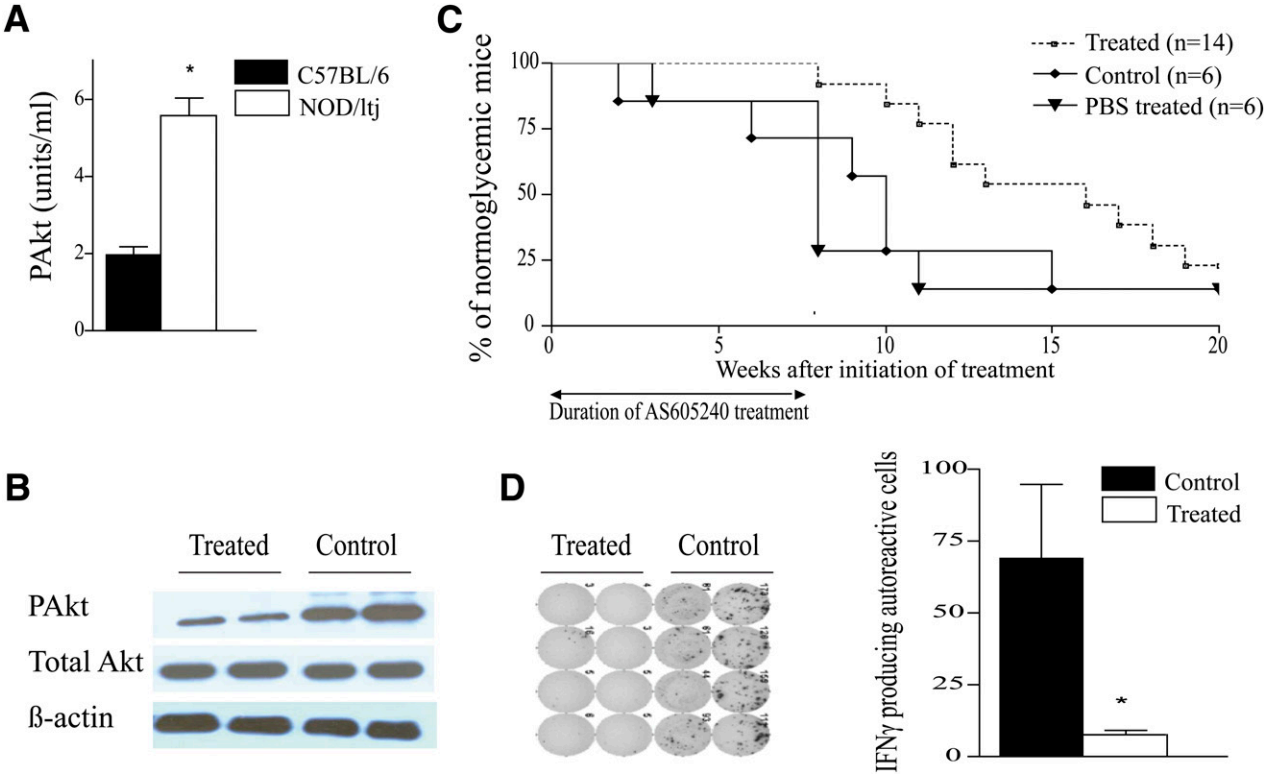

FIG. 1. AS605240 suppresses intracellular PAkt in splenocytes of NOD mice and delays diabetes onset. *A*: PAkt measurement by an ELISA assay of lysates from splenocytes of 12-week-old C57BL/6 and NOD mice shows higher levels of PAkt in NOD mice (*$P < 0.05$; $n = 4$ mice in each group). *B*: Western blot analysis of lysates from splenocytes of NOD mice treated with either AS605240 (30 mg/kg) or PBS control for 7 days ($n = 3$ mice in each group). *C*: Kaplan-Meier cumulative survival of NOD mice treated with AS605240 starting at 10 weeks of age showed 100% prevention for the duration of treatment of 7 weeks. The difference remains significant up to 15 weeks postinitial treatment ($P < 0.05$; $n = 12$–15 mice in each group). *D*: Representative example of IFN-γ ELISpot analysis after an ex vivo BDC2.5 pancreatic-peptide challenge of splenocytes isolated from normoglycemic NOD mice treated for 3 weeks compared with age-matched control NOD mice. Bar graph represents the frequency of IFN-γ–producing autoreactive cells (*$P < 0.05$; $n = 4$ mice in each group). Results are presented as the mean ± SEM. (A high-quality color representation of this figure is available in the online issue.)

AS605240 prevents autoimmune diabetes in prediabetic NOD mice. Ten-week-old prediabetic NOD mice were injected with 30 mg/kg of AS605240 i.p. daily for 7 weeks. As shown in Fig. 1*C*, AS605240 conferred 100% protection during the course of 7 weeks of therapy. Following discontinuation of therapy, 50 and 25% of the NOD mice remained free from diabetes at 25 and 30 weeks of age, respectively. No survival difference was observed in the NOD mice treated with the same volume of PBS (vehicle for the AS605240) as compared with untreated control ($P = 0.7$; $n = 6$ in each group). Histopathological analysis of the pancreatic islet morphology and infiltration was also performed at 3 and 10 weeks postinitial treatment on control and treated animals ($n = 4$ mice/group). The AS605240-treated NOD mice had well-preserved islets with strong insulin staining at 3 weeks postinitial treatment and a significantly lower insulitis score, whereas substantial islet infiltration was observed in untreated mice (Supplementary Fig. 2). We assessed the activity of autoreactive $CD4^+$ T cells by measuring cytokine patterns after a BDC2.5-pancreatic-peptide challenge of splenocytes recovered from AS605240-treated and untreated NOD mice at 3 and 10 weeks postinitial treatment as previously described (19). Treated mice had a significantly lower frequency of autoreactive IFN-γ–producing $CD4^+$ cells compared with untreated NOD mice after 3 weeks of treatment ($P = 0.02$) (Fig. 1*D*). At 20 weeks of age, AS605240-treated NOD mice showed minimal infiltration compared with the age-matched untreated control mice (Fig. 2*A*). Insulitis scoring was performed, which showed a significantly lower grade of insulitis in the AS605240-treated mice compared with the untreated NOD age-matched groups (Fig. 2*B*).

AS605240 suppresses autoreactive T cells while increasing Tregs in NOD mice. An enzyme-linked immunospot (ELISpot) assay on recovered splenocytes stimulated with BDC2.5-peptide ex vivo showed that treated animals had significantly lower frequency of autoreactive IFN-γ–producing $CD4^+$ cells compared with untreated NOD mice at 10 weeks postinitial treatment ($P = 0.02$) (Fig. 2*C*). Similarly, Luminex was used on supernatant collected from the ELISpot assay to measure various cytokines and chemokines involved in the pathogenesis of T1D. Our data showed marked suppression of inflammatory cytokines including Th1, Th2, and Th17 cells as well as IFN-γ–inducible protein-10, monocyte chemoattractant protein-1, and regulated on activation, normal T cell expressed and secreted chemokine secretion at 20 weeks of age (Fig. 2*D*). Flow cytometric analysis of splenocytes showed a decrease in the absolute number of effector $CD4^+$ and $CD8^+$ T cells identified as $CD44^{high}CD62L^{low}$ at 10 weeks post-initial treatment (Fig. 2*E*), which was concurrent with a significant increase in the percentage of regulatory $CD4^+CD25^+FoxP3^+$ cells in spleens of treated versus untreated mice ($16.55 \pm 1.6\%$ vs. $9.84 \pm 1.3\%$, respectively; $P = 0.02$) (Fig. 2*F* and *G*), with a tendency toward statistical significance in the absolute number ($1.62 \pm 0.19 \times 10^6$ vs. $1.28 \pm 0.05 \times 10^6$, respectively; $P = 0.07$) (Fig. 2*E*). Of note, no difference was observed in the percentage of plasmacytoid dendritic cells defined as $CD11c^+CD11b^-B220^+$ in the spleens of treated mice compared with control mice at 20 weeks of age ($0.76 \pm 0.09\%$ vs. $0.73 \pm 0.09\%$; $P = 0.4$).

AS605240 suppresses autoreactive T cells in vitro. Stimulating $CD4^+$ BDC2.5 T cells with BDC2.5-peptide in vitro in the presence of AS605240 showed a dose-dependent suppression of autoreactive $CD4^+$ T-cell proliferation in vitro (Fig. 3*A*) and production of IFN-γ in an ELISpot assay (Fig. 3*B*). We also examined the effect of PI3Kγ inhibition on the production of cytokines and chemokines pertinent to the pathogenesis of T1D by subjecting supernatant from the ELISpot to a Luminex assay (22). Autoreactive T cells treated with AS605240 also produced fewer multiple inflammatory cytokines such as IL-6 and IL-17 and chemokines such as IFN-γ–inducible protein-10 and monocyte chemoattractant protein-1 as shown in Fig. 3*C*. Adding IFN-γ (4 ng/mL), IL-2 (2 ng/mL), IL-6 (2 ng/mL), IL-17 (10 ng/mL), or a combination of these cytokines to the autoreactive assay failed to restore proliferation of the $CD4^+$ BDC2.5 T cells inhibited by AS605240 (data not shown). Furthermore, we investigated whether AS605240 caused an increased rate of T-cell death, which in turn could provide an explanation for the lack of activation. No increase in cell death (positive for 7AAD and Annexin) or apoptosis (positive for Annexin and negative for 7AAD) was observed in $CD4^+$ T cells treated with AS605240 (Supplementary Fig. 3).

AS605240 results in the expansion of Tregs. We then assessed the effects of inhibiting the $CD4^+$ T cell PI3Kγ pathway on Treg generation in vitro. A total of 2.5×10^5 $CD4^+$ T cells from NOD mice were cultured for 72 h in a Treg-generation assay, as described previously, using anti-CD3/CD28 stimulation and TGF-β with and without AS605240 (23,24). Flow cytometric analysis for $CD4^+CD25^+FoxP3^+$ revealed a significant increase of $FoxP3^+$ cells treated with AS605240 compared with untreated cells stimulated with anti-CD3/CD28 and TGF-β as measured by percentage (Fig. 3*D*) and absolute number ($12 \pm 1.72 \times 10^3$ vs. $6.1 \pm 1.5 \times 10^3$, respectively; $P = 0.02$). However, no difference in Tregs was observed when the PI3Kγ-i was added to $CD4^+$ T cells stimulated with anti-CD3/CD28 in the absence of TGF-β, as measured by percentage (Fig. 3*D*) and absolute number ($2.97 \pm 0.54 \times 10^3$ vs. $3.46 \pm 0.64 \times 10^3$, respectively; $P = 0.2$). No significant increase in $FoxP3^+$ cells was observed when $CD25^+$-depleted $CD4^+$ T cells were treated with AS605240 compared with control (anti-CD3/CD28 and TGF-β) (data not shown). For the in vivo analysis, 10×10^6 BDC2.5 splenocytes with and without $CD25^+$ depletion were injected into the tail vein of NOD-*scid* mice. Both conditions were either treated by daily i.p. injections of 30 mg/kg AS605240 or left untreated. Results showed a significantly increased $CD4^+CD25^+FoxP3^+$ Treg population in the spleen 7 days posttransfer of BDC2.5 splenocytes in the treated group compared with control by percentage analysis ($22.73 \pm 3.47\%$ vs. $12.54 \pm 0.60\%$, respectively; $P = 0.02$) and absolute count ($3.80 \pm 1.47 \times 10^5$ vs. $0.83 \pm 0.29 \times 10^5$, respectively; $P = 0.05$). However, no significant increase in the $CD4^+CD25^+FoxP3^+$ Treg population was observed after injection of $CD25^+$-depleted splenocytes whether they were followed by treatment or not (Fig. 3*E*).

cAMP response element-binding signaling is responsible for the expansion of Tregs under PI3Kγ inhibition. We then examined cell lysates from $CD4^+$ T cells retrieved from the in vitro Treg-generation assay described above using anti-CD3/CD28 and TGF-β with or without PI3Kγ-i by an 8-plex Multi-Pathway Signaling Kit-Phosphoprotein (Milliplex MAP Kit; Millipore). We found that the addition of PI3Kγ-i increased the expression of phosphorylated cAMP response element-binding (CREB) compared with control (anti-CD3/CD28 and TGF-β). No differential increase was noted in the expression of extracellular signal–related kinase/mitogen-activated protein kinase, signal transducer and activator of transcription (STAT) 3,

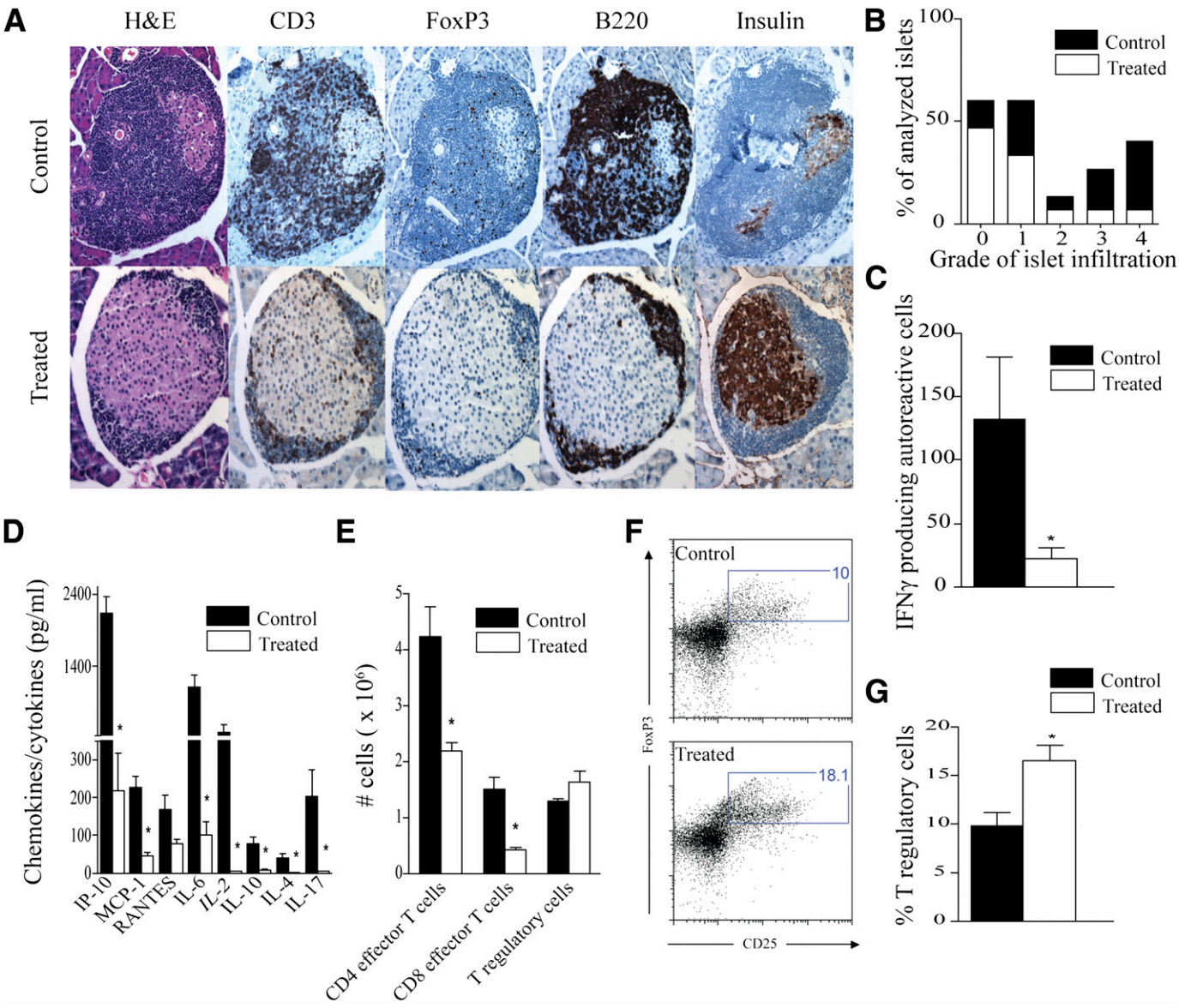

FIG. 2. Prediabetic NOD mice were treated with AS605240 for 7 weeks beginning at 10 weeks of age. *A*: Representative example of pancreatic histology from AS605240-treated group and untreated control at 20 weeks of age. Insulitis score at 20 weeks of age measured on 30 different islets from four mice per group is presented in *B*. IFN-γ ELISpot analysis (*C*) and Luminex assay on supernatant (*D*) from an ex vivo BDC2.5-pancreatic-peptide challenge of splenocytes recovered from AS605240-treated mice compared with control NOD mice at 20 weeks of age (*$P < 0.05$, $n = 4$ mice in each group). *E*: Flow cytometry analysis on splenocytes from treated mice at 20 weeks of age shows significant suppression of the absolute count of CD4 effector T cells ($CD4^+CD44^{high}CD62L^{low}$) and CD8 effector T cells ($CD8^+CD44^{high}CD62L^{low}$) while sparing Tregs ($CD4^+CD25^+FoxP3^+$) compared with control (*$P < 0.05$; $n = 4$ mice in each group). *F*: Representative example of FACS staining from splenocytes of treated and control NOD mice at 20 weeks of age shows higher percentage of Tregs ($CD4^+CD25^+FoxP3^+$) in treated compared with control mice. *G*: Bar graph shows the percentage of Tregs analyzed by flow cytometry in splenocytes of treated mice compared with control at 20 weeks of age (*$P < 0.05$; $n = 4$ mice in each group). Results are presented as the mean ± SEM. (A high-quality digital representation of this figure is available in the online issue.)

inhibitory NF-κBα, Jun NH_2-terminal kinase, STAT5A/B, P70 S6 kinase, and p38 (Fig. 4*A*). CREB, a nuclear transcription factor responsible for cell survival and proliferation, was recently shown to increase FoxP3 transcription by binding to its promoter (25). We then examined the effect of CREB inhibitor on Tregs generation in our assay (26). Addition of PI3Kγ-i–expanded Tregs significantly compared with control (anti-CD3/CD28 and TGF-β) (30.40 ± 2% vs. 14.65 ± 2.4%, respectively; $P = 0.04$). However, the addition of CREB inhibitor at 40 μmol/L to anti-CD3/CD28, TGF-β, and PI3Kγ-i suppressed Treg generation compared with anti-CD3/CD28, TGF-β, and PI3Kγ-i (5.05 ± 0.7% vs. 30.40 ± 2%, respectively; $P = 0.04$, Fig. 4*B* and *C*). Furthermore, addition of the same concentration of CREB inhibitor to anti-CD3/CD28 and TGF-β had no significant effect on Treg generation compared with control (18.43 ± 3.3% vs. 14.65 ± 2.4%, respectively; $P = 0.5$; Fig. 4*B* and *C*). No increase in cell death (positive for 7AAD and Annexin) or apoptosis (positive for Annexin and negative for 7AAD) was observed in $CD4^+$ T cells treated with CREB inhibitor (data not shown).

AS605240 treatment reverses hyperglycemia in newly hyperglycemic NOD mice. For reversal studies, NOD mice were observed for the development of hyperglycemia (>250 mg/dL). After two consecutive hyperglycemic

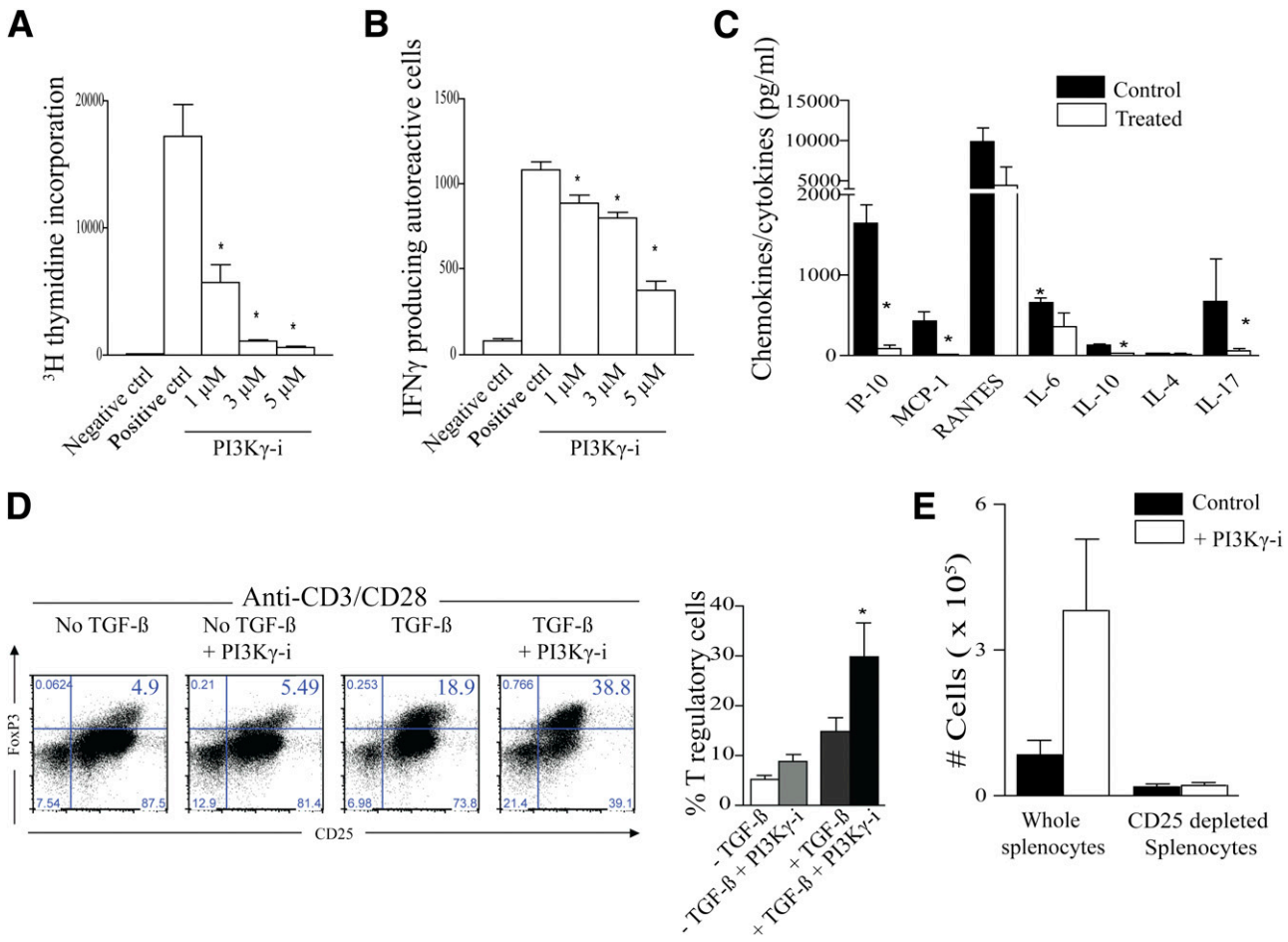

FIG. 3. AS605240 suppressed in a dose-dependent manner the proliferation of BDC2.5 CD4$^+$ T cells stimulated by the BDC2.5-pancreatic-peptide in vitro as measured by thymidine incorporation (*A*) and their production of IFN-γ in an ELISpot assay (*B*) (P* < 0.05, *n* = 3–5 mice; data are representative of three separate experiments). The negative control (ctrl) splenocytes received no peptide stimulation, whereas the positive control cells were stimulated with the BDC2.5-peptide. *C*: Luminex assay was used on supernatant collected from the ELISpot assay. AS605240 potently suppressed inflammatory cytokines and chemokines produced by BDC2.5 CD4$^+$ T cells stimulated by the BDC2.5-pancreatic-peptide in vitro (**P* < 0.05; *n* = 3–5 mice; data are representative of two separate experiments). *D*: Representative example of FACS staining shows the effect of the AS605240 on Treg generation in vitro using a CD3/CD28 stimulation assay with and without TGF-β. Cells are gated on CD4$^+$ T cells. Data represent one of three separate experiments. The bar graph represents the percentage of Tregs from these experiments (**P* < 0.05; *n* = 3–5 mice; data are representative of three separate experiments). *E*: Bar graph shows the absolute counts of Tregs in the spleen of NOD-*scid* mice that received an adoptive transfer of either whole BDC2.5 splenocytes or CD25$^+$ depleted BDC2.5 splenocytes, followed by treatment with AS605240 for 7 days, as compared with untreated control receiving an adoptive transfer (**P* < 0.05; *n* = 4 mice in each group). Results are presented as the mean ± SEM. (A high-quality color representation of this figure is available in the online issue.)**

measurements were taken within 24 h, NOD mice were given 30 mg/kg of AS605240 i.p. daily for 3 weeks. None of the hyperglycemic NOD mice treated i.p. with PBS showed reversal of hyperglycemia (Fig. 5*A*). We observed diabetes reversal in 73% of AS605240-treated NOD hyperglycemic mice by the end of the 3 weeks of treatment (11 out of 15 treated hyperglycemic NOD mice). Twenty-five percent of mice showed long-standing reversal of diabetes following the discontinuation of AS605240 (Fig. 5*B*). Notably, an extended 8-week treatment regimen resulted in an initial reversal rate of 80% in the diabetic mice (four out of five mice) and normoglycemia for at least 13 weeks post-initial treatment in the reversed-treated mice. Three out of the four mice were still normoglycemic >10 weeks after stopping administration of AS605240 (Fig. 5*C*). Histological analysis of untreated NOD mice after 3 weeks postonset of hyperglycemia showed necrotic islets with negative-staining insulin. In contrast, treated mice showed a lower percentage of infiltrates confined to the border of islets, positive FoxP3 cells, and strong staining for insulin (Supplementary Fig. 4).

AS605240 treatment reverses hyperglycemia in early diabetic NOD mice through Tregs. Reversal NOD mice at 100 days postreversal had a significant increase in peripheral Tregs compared with age-matched diabetic NOD mice (Fig. 5*D*). To ensure the functionality of Tregs, 20 × 10^6 splenocytes (with and without CD25 depletion) from normoglycemic reversed NOD mice treated with AS605240 or untreated hyperglycemic NOD mice were adoptively transferred into NOD-*scid* mice. The control groups receiving whole splenocytes and CD25-depleted splenocytes from early diabetic NOD mice developed diabetes at 3 to 4 weeks of age. Likewise, mice receiving cells from nondiabetic 12-week-old NOD mice developed diabetes 3–5 weeks later. In comparison, mice injected with undepleted splenocytes obtained from reversed-treated NOD mice developed diabetes after 6–8 weeks, thus delaying diabetes onset by an additional 3–5 weeks when compared with mice receiving adoptive transfer of splenocytes from diabetic NOD mice. Depletion of CD25$^+$ cells in the splenocytes of reversed mice abrogated the delay in diabetes

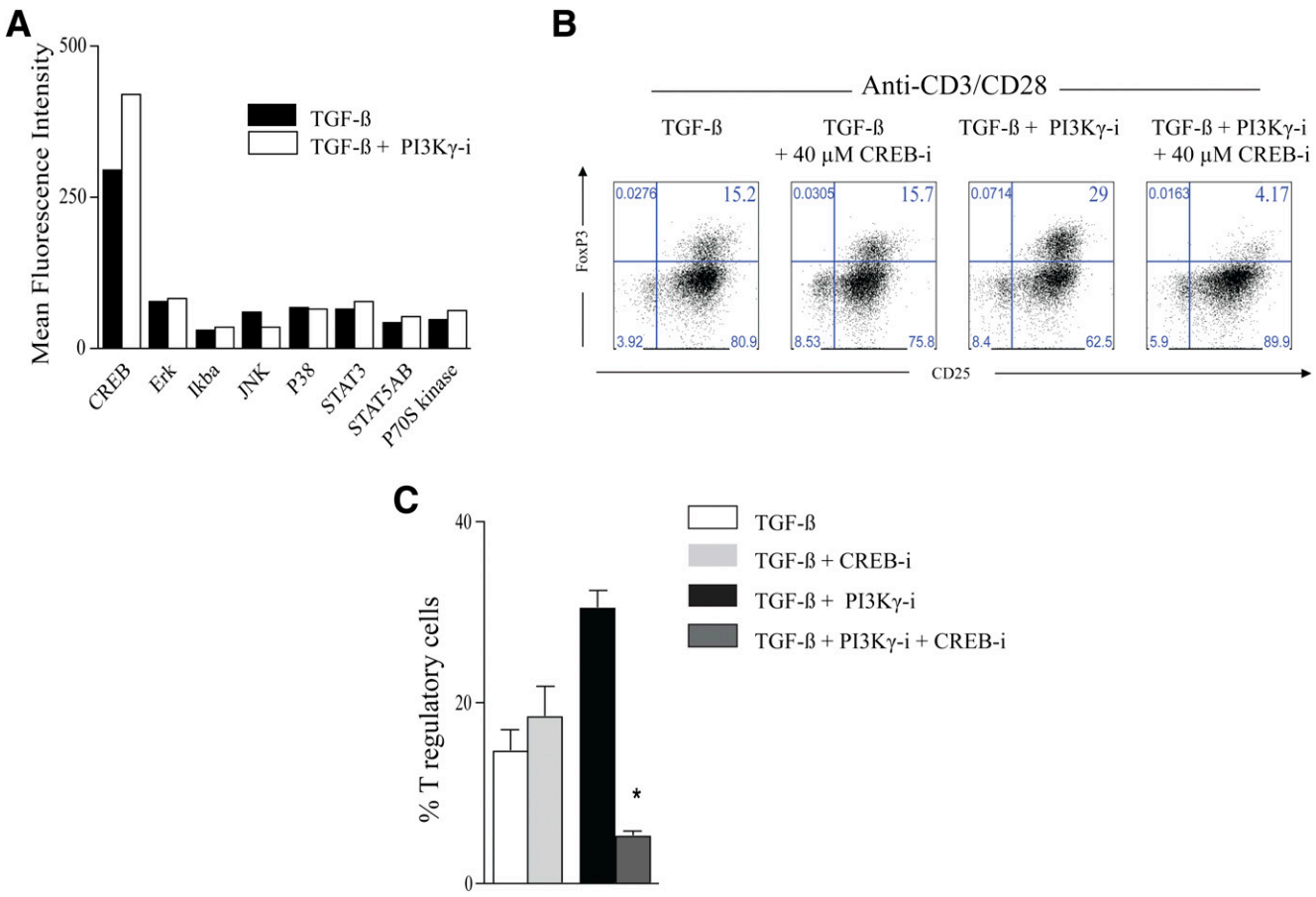

FIG. 4. ***A*: Cell lysate analysis by Luminex assay of CD4$^+$ T-cells retrieved from the in vitro Treg-generation assay (anti-CD3/CD28 stimulation and TGF-β) at 20 min showed an increase in the phosphorylation of the nuclear transcription factor CREB under PI3Kγ pathway inhibition compared with untreated control (data represent one of three separate experiments). *B*: Representative example of FACS staining showing the effect of the CREB inhibition on Treg generation in vitro using a CD3/CD28 stimulation assay with TGF-β with or without PI3Kγ-i (data represent one out of three separate experiments). The percentages of Tregs from these different conditions are shown in the bar graph in *C* (*$P < 0.05$; n = 3–5 mice; data are representative of three separate experiments). Results are presented as the mean ± SEM. (A high-quality color representation of this figure is available in the online issue.)**

onset. As shown in Fig. 5*E*, injection of CD25$^+$ depleted splenocytes from reversed NOD mice led to the development of diabetes within 3 weeks postinjection.

AS605240 treatment suppresses T-cell infiltration in pancreatic islets while increasing Tregs. FACS analysis of lymphocytes isolated from pancreata of reversed mice 3 weeks after daily treatment with PI3Kγ-i shows significant suppression of CD4$^+$ and CD8$^+$ T cells infiltrating the pancreas in treated compared with PBS-treated mice (Fig. 6*A* and *B*). The percentage of CD4$^+$ T cells in treated mice expressing FoxP3 as a marker of Tregs were significantly higher compared with PBS-treated mice (57.88 ± 7.84% vs. 17.87 ± 5.60%, respectively; $P = 0.006$) (Fig. 6*C*). No difference was observed in the Treg absolute count between treated and control mice ($21.12 \pm 6.29 \times 10^3$ vs. $18.36 \pm 6.00 \times 10^3$, respectively; $P = 0.7$). Of note, no difference was observed in the absolute number of dendritic cells in the pancreas between treated and PBS-treated mice (15330 ± 37 vs. 16150 ± 54, respectively; $P = 0.91$). No difference was observed in the pancreatic lymph nodes ($89.75 \pm 26.54 \times 10^3$ vs. $67.24 \pm 10.54 \times 10^3$, respectively; $P = 0.46$)

PI3Kγ inhibition suppresses the expression of PAkt (Ser^{473}) in splenocytes of reversed mice. Spleens from PI3Kγ-i–treated and PBS-treated NOD mice were subjected to phospho-FACS analysis. AS605240 treatment significantly reduced CD4$^+$ and CD8$^+$ T cells expressing high levels of PAkt (Ser^{473}) in reversed NOD mice 3 weeks posttreatment (Fig. 6*D* and *E*). Tregs from spleens of treated or control mice, defined as CD4$^+$CD25$^+$FoxP3$^+$, expressed lower levels of intracellular PAkt (Ser^{473}) compared with effector cells, defined as CD4$^+$CD25$^+$FoxP3$^-$ (Fig. 6*F*).

Establishing PI3Kγ inhibition-based strategies to reverse T1D. Given the overt toxicity and lack of efficacy of monotherapeutic strategies, the need for developing combinatorial strategies is more pressing than ever before (27). We tested the combination of PI3Kγ inhibition with one of the most clinically relevant immunomodulatory agents, anti-CD3 (28). We treated our hyperglycemic mice (defined as above) with a combination of AS605240 and anti-CD3 with one group receiving a single dose of anti-CD3 (12.5 μg) i.p. at the onset of hyperglycemia and the other receiving additional daily injections of AS605240 (30 mg/kg) i.p. daily for 3 weeks. As shown in Fig. 7*A*, none of the hyperglycemic anti-CD3–treated NOD mice showed reversal of hyperglycemia. However, our combinatorial protocol resulted in hyperglycemia reversal in 67% of the treated NOD mice (four out of six mice). All of the treated mice maintained normoglycemia for at least 13 weeks following the initiation of treatment (Fig. 7*B*). Finally, as mammalian

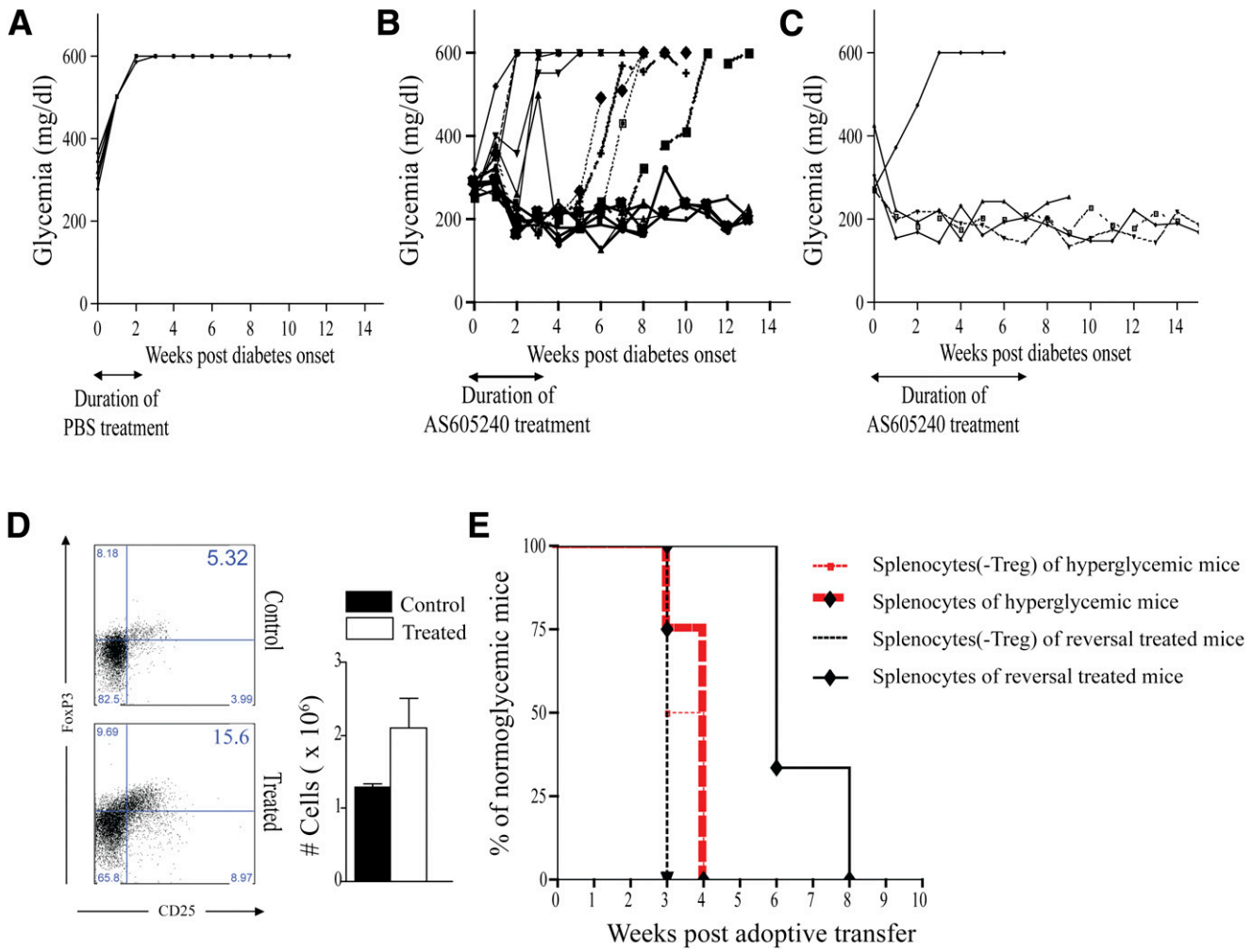

FIG. 5. ***A*: Blood glucose of PBS-treated early diabetic NOD mice shows absence of reversal in 100% of the mice (n = 7 mice). *B*: Blood glucose of treated early diabetic NOD mice with 30 mg/kg of AS605240 shows a 73% rate of reversal at 3 weeks post-start of treatment that becomes 25% at 13 weeks post-start of treatment (n = 14 mice). *C*: Blood glucose of treated early diabetic NOD mice with 30 mg/kg of AS605240 for 8 weeks shows 80% reversal at 10 weeks post-start of treatment (n = 5 mice). *D*: Representative example of FACS staining from splenocytes of treated reversal mice and age-matched diabetic NOD mice. Bar graph shows the absolute count of Tregs analyzed by flow cytometry in splenocytes of treated reversal mice compared with age-matched diabetic NOD mice (*P < 0.05; n = 4 mice in each group). *E*: Kaplan-Meier cumulative survival curves of diabetes onset in NOD-*scid* mice that received splenocytes harvested from treated reversal mice with or without CD25 depletion or from early diabetic control mice with or without CD25 depletion. Depleting Tregs prior to transfer of splenocytes into NOD-*scid* mice abrogates the delay in inducing diabetes by the splenocytes of reversal mice. No difference in diabetes onset was observed in NOD-*scid* mice that received splenocytes from early diabetic control mice with or without CD25 depletion (n = 3 to 4 mice in each group). Results are presented as the mean ± SEM. (A high-quality color representation of this figure is available in the online issue.)**

target of rapamycin (mTOR) is downstream of the PI3K pathway, we were interested in comparing the therapeutic efficacy of rapamycin to that of AS605240 in early diabetic NOD mice. Hyperglycemic NOD mice were given 1 mg of rapamycin i.p. at days 0, 2, 4, 6, 8, and 10. As shown in Fig. 7*C*, none of the hyperglycemic NOD mice treated with rapamycin showed reversal of hyperglycemia.

DISCUSSION

There has been a significant increase in the incidence of T1D worldwide, rendering the disease a major global health care problem with no currently available curative therapy (12). Although clinical trials using known immunosuppressants have yielded promising results in preventing T1D, they have not met expectations due to their inadequacy and serious morbidity (13,29). This has prompted investigators to search for alternatives. In this regard, the PI3K pathway is an attractive target for T1D therapy. Among the various classes of PI3Ks, PI3Kγ is expressed mainly in leukocytes (8). The role of PI3Kγ in thymocyte survival and activation of mature T cells was first highlighted in mice lacking the p110 catalytic subunit of PI3Kγ (7,30,31). Barber et al. (32) has shown that deletion of the PI3K–PKB pathway, downstream of PI3Kγ, decreases survival of pathogenic $CD4^+$ memory cells in mouse models of SLE. PI3Kγ has also been shown to play a critical role in the downstream signaling of TCR-mediated T-cell activation (5). The PI3Kγ pathway has also been shown to play a critical role in the chemotaxis of leukocytes as well (8,33). Although a growing body of work has highlighted the role of anti-PI3Kγ strategies in various diseases, the role of such therapy in T1D is unknown (8,9,16,34–36).

In this report, we have examined the immunoregulatory function of AS605240 in regulating T1D. We observed a significant activation of the PI3K–PKB pathway in the splenocytes of diabetic NOD mice compared with the splenocytes of C57BL/6 mice. AS605240 prevented T1D in

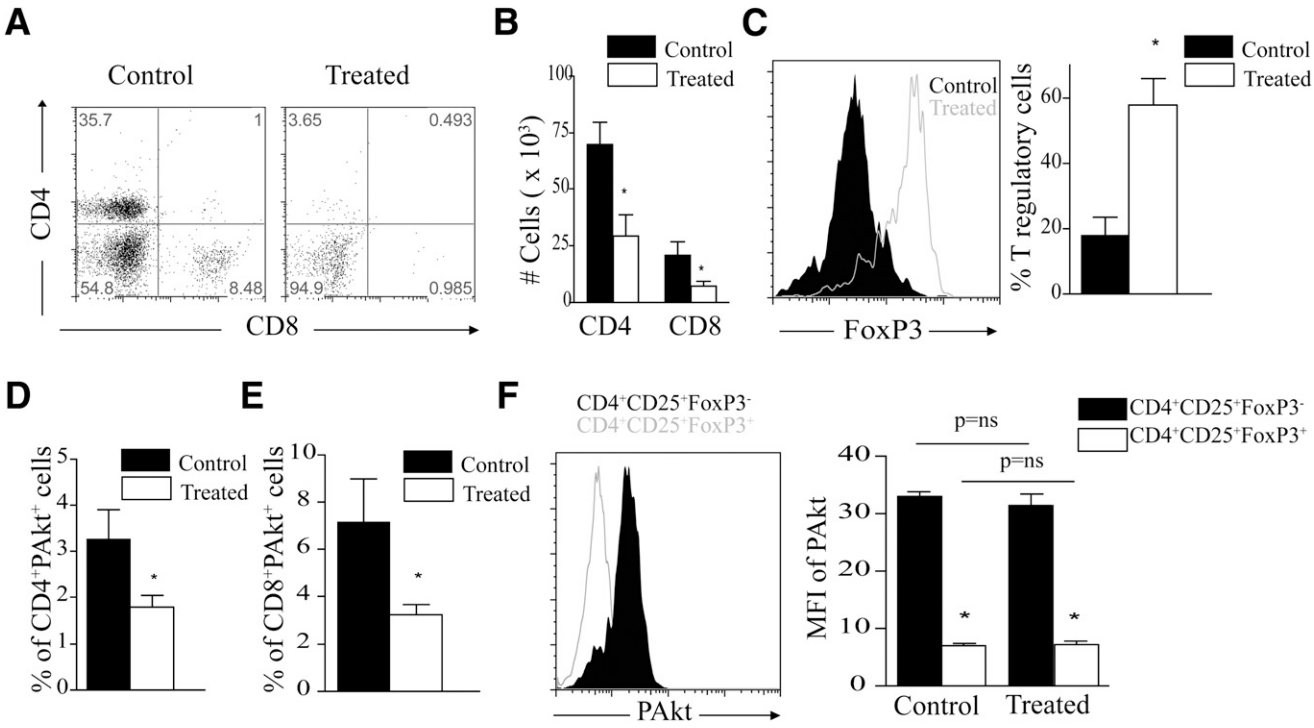

FIG. 6. ***A*****: Representative example of FACS staining of cells isolated from pancreas of NOD mice treated with either AS605240 or PBS vehicle for 3 weeks. Dot plots show gating on CD4⁺ and CD8⁺ T cells.** ***B*****: The bar graph represents the absolute number of CD4⁺ and CD8⁺ T cells in the PI3Kγ-i–treated mice compared with control (*$P < 0.05$; $n = 3$ to 4 mice in each group).** ***C*****: Representative example of FACS staining of cells isolated from pancreas of NOD mice treated with either AS605240 or PBS vehicle. Cells are gated on CD4⁺ T cells and show FoxP3 expression. Bar graph represents the percentage of Tregs in cells isolated from pancreas of PI3Kγ-i–treated mice compared with control PBS-treated NOD mice (*$P < 0.05$; $n = 3$ to 4 mice in each group).** ***D*****: Bar graph represents the percentage of CD4⁺ T cells highly expressing PAkt by flow cytometry in spleens of PI3Kγ-i–treated mice compared with control PBS-treated mice (*$P < 0.05$; $n = 3$ to 4 mice in each group).** ***E*****: Bar graph represents the percentage of CD8⁺ T cells highly expressing PAkt (*$P < 0.05$; $n = 3$ to 4 mice in each group).** ***F*****: Representative example of FACS staining of PAkt expression in CD4⁺CD25⁺FoxP3⁺ Tregs compared with CD4⁺CD25⁺FoxP3⁻ non-Tregs in splenocytes of treated NOD mice. Bar graph shows the mean fluorescence intensity (MFI) of PAkt expression in CD4⁺CD25⁺FoxP3⁺ Tregs compared with CD4⁺CD25⁺FoxP3⁻ non-Tregs in splenocytes of NOD mice treated with either AS605240 or PBS vehicle (control) (*$P < 0.05$; $n = 3$ to 4 mice in each group). Results are presented as the mean ± SEM.**

100% of prediabetic NOD mice during the course of therapy. Although PI3Kγ inhibition potently abrogated autoreactive T cells, it spared Tregs. Importantly, AS605240 increased the ratio of Tregs to effector populations in the treated mice, tipping the balance from autoreactive T cells to Tregs, thus conferring protection against autoimmune diabetes. This ratio has been reported to be central to the suppression of autoreactive T cells (37). Ablation of Tregs in the BDC2.5/NOD mouse model of autoimmune diabetes leads to accelerated disease development (38). PI3Kγ inhibition suppressed autoreactive T cells along with chemokines and inflammatory cytokines shown to play a role in the pathogenesis of T1D in vitro and in vivo (22,39–41). Moreover, we showed that PI3Kγ inhibition results in increased Tregs in vitro and in vivo. We then studied signaling pathways known to induce FoxP3 expression, including extracellular signal–related kinase/mitogen-activated protein kinase, STAT3, P70 S6 kinase, inhibitory NF-κBα, CREB, Jun NH_2-terminal kinase, STAT5A/B, and p38 (25,42–48). Phosphorylated CREB was elevated in CD4⁺ T cells treated with PI3Kγ-i in our Treg generation assay. This increase was associated with higher Treg generation, whereas the inhibition of CREB was associated with Treg suppression. This suggests that PI3Kγ inhibition may act on Treg generation through the CREB pathway. The more pronounced suppression of Tregs generation observed in the PI3Kγ-i group compared with control could be related to the interaction of PI3K and CREB on T-cell activation and the synergistic suppressive effect of their inhibitors on T-cell function. Although the role of Akt in the expression of FoxP3 is described, the downstream mechanisms involved in FoxP3 transcription are not well known (49). Our data provide new insights on the interplay between the PI3Kγ pathway and the CREB pathway in the induction of FoxP3 transcription and its application in T1D.

Achieving effective and durable reversal of T1D has been very challenging, and finding a cure is extremely desirable. AS605240 reversed T1D in ~80% of early diabetic NOD mice. In accordance with our in vitro data, Tregs were found to be increased in the spleen of treated reversal NOD mice compared with control NOD mice of the same age. Moreover, the pancreas of treated reversal NOD mice showed significant suppression of CD4⁺ and CD8⁺ T cells compared with PBS-treated mice. Interestingly, the remaining CD4⁺ T cells in treated mice mostly expressed FoxP3, a marker of Tregs, compared with PBS-treated mice. Our data indicate that expression of PAkt was preferentially higher in effector T cells. Notably, CD4⁺ effector T cells had significantly higher levels of PAkt compared with Tregs in treated and control mice. Treated reversal mice also showed significant reduction in CD4⁺ and CD8⁺ T cells expressing high levels of PAkt (Ser^{473}) compared with PBS-treated controls. Our data suggest that the level of PAkt in an individual cell will determine its function as an effector or regulatory cell and that inhibition of PAkt will tip the balance from effector to regulatory cell.

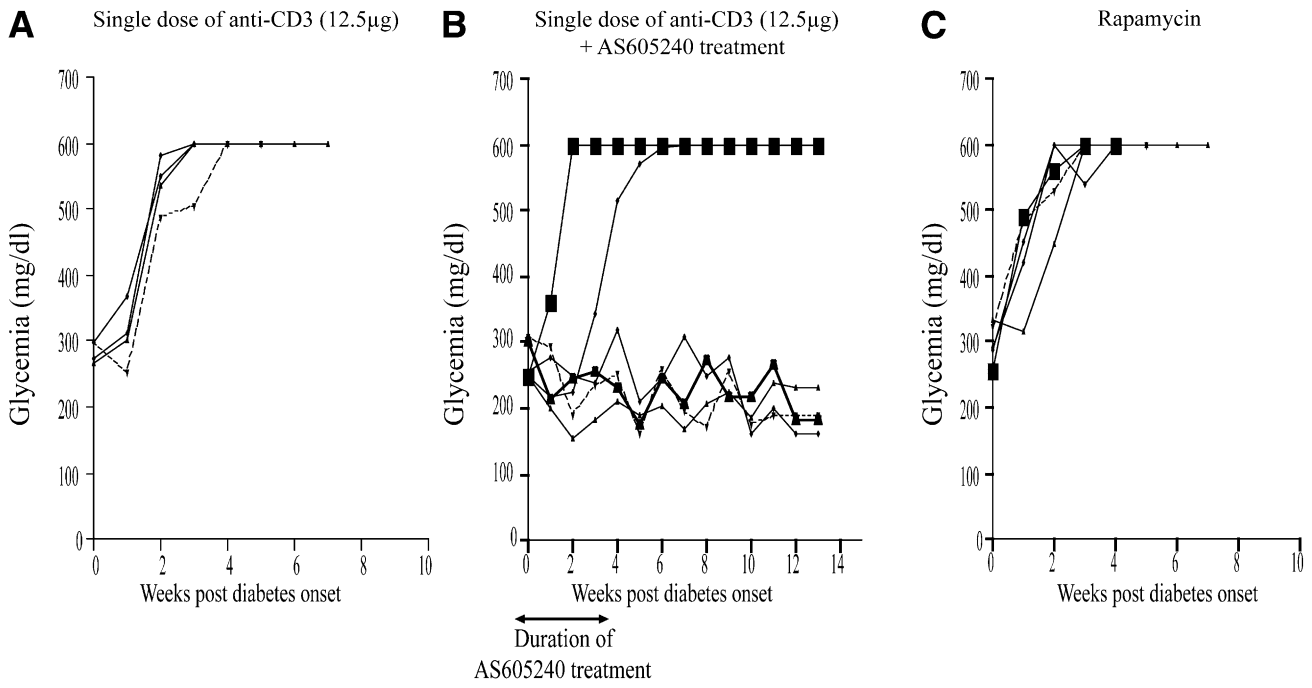

FIG. 7. ***A*****: Blood glucose of early diabetic NOD mice treated with a single low-dose anti-CD3 (12.5 μg) shows no therapeutic effect in any of the treated mice (*n* = 4 mice).** ***B*****: Blood glucose of early diabetic NOD mice treated with a single low-dose anti-CD3 (12.5 μg) and 30 mg/kg of AS605240 for 3 weeks shows long-term reversal in ~70% of mice (*n* = 6 mice).** ***C*****: Blood glucose of rapamycin-treated early diabetic NOD mice shows no reversal of hyperglycemia (*n* = 5 mice).**

To test the functionality of Tregs in maintaining tolerance to self-antigens in our system, at 100 days, we adoptively transferred splenocytes with and without Tregs from the treated reversed mice into NOD-*scid* mice. As compared with the splenocytes from early diabetic NOD mice, splenocytes from reversal-treated mice induced hyperglycemia later in NOD-*scid* mice. Depleting Tregs in splenocytes of the reversal mice abrogated this delay.

Major efforts are now underway to explore various options to further improve the outcome of combinational therapies (27). Anti-CD3 was reported to reverse diabetes in 75–80% of early diabetic NOD mice (50,51). Furthermore, anti-CD3 administered to patients with new-onset T1D preserved residual β-cell function for at least 18 months. However, the majority of patients treated with anti-CD3 had significant adverse events (52). A combination of a short-duration PI3Kγ inhibition therapy and low-dose anti-CD3 could overcome those limitations and constitute a novel promising therapeutic strategy. To address the potential role of mTOR blockade in reversing T1D, we show that rapamycin does not reverse T1D, a result in concordance with previous reports (53). Interestingly, Valle et al. (51) have shown that rapamycin has a deleterious effect on T1D by breaking the anti-CD3–induced tolerance in NOD mice. These data indicate that blockade of mTOR does not play the major role in the antidiabetic effect of PI3Kγ inhibition observed in this study.

It should be noted that future efforts are underway to develop inhibitors with greater specificity to the PI3Kγ subunit. Although AS605240 has been demonstrated to be specific to the PI3Kγ subunit, we cannot rule out minimal interaction with other subunits. Finally, whether the higher level of PAkt in NOD splenocytes relative to C57BL/6 splenocytes is due to an inherent activation of the PI3K pathway in NOD lymphocytes or due to the increased frequency of pathogenic T cells remains an interesting question for future studies.

In summary, these results provide vital preclinical data to support the concept of translating PI3Kγ inhibition therapy to patients with T1D.

ACKNOWLEDGMENTS

This work is supported by Juvenile Diabetes Research Foundation Grant 4-2007-1065 and a Juvenile Diabetes Research Foundation Regular Grant (to R.A.).

No other potential conflicts of interest relevant to this article were reported.

J.A. designed and performed experiments, analyzed and interpreted data, and drafted the manuscript. R.F.M. performed experiments, analyzed data, and revised the manuscript. W.E., M.M., N.E.H., S.Y., M.J., A.T., and A.P. performed experiments and analyzed data. P.F., T.R., and R.A. helped with the study design, interpreted the data, and critically revised and finalized the manuscript. R.A. is the guarantor of this work and, as such, had full access to all of the data in the study and takes responsibility for the integrity of the data and the accuracy of the data analysis.

Parts of this study were presented at the 70th Scientific Sessions of the American Diabetes Association, Orlando, Florida, 25–29 June 2010.

The authors thank Bechara Mfarrej and Peter Jindra from the Renal Division at Brigham and Women's Hospital, Youmna Lahoud from the Center for Neurologic Diseases at Brigham and Women's Hospital, and Scott Rodig from the Department of Pathology at Brigham and Women's Hospital for technical support. They also thank Mohammed H. Sayegh from the Renal Division at Brigham and Women's Hospital for comments and critical reading of the manuscript.

REFERENCES

1. Rückle T, Schwarz MK, Rommel C. PI3Kgamma inhibition: towards an 'aspirin of the 21st century'? Nat Rev Drug Discov 2006;5:903–918
2. Brunet A, Bonni A, Zigmond MJ, et al. Akt promotes cell survival by phosphorylating and inhibiting a Forkhead transcription factor. Cell 1999;96:857–868
3. Vanhaesebroeck B, Leevers SJ, Ahmadi K, et al. Synthesis and function of 3-phosphorylated inositol lipids. Annu Rev Biochem 2001;70:535–602
4. Walker EH, Perisic O, Ried C, Stephens L, Williams RL. Structural insights into phosphoinositide 3-kinase catalysis and signalling. Nature 1999;402:313–320
5. Alcázar I, Marqués M, Kumar A, et al. Phosphoinositide 3-kinase gamma participates in T cell receptor-induced T cell activation. J Exp Med 2007; 204:2977–2987
6. Deane JA, Fruman DA. Phosphoinositide 3-kinase: diverse roles in immune cell activation. Annu Rev Immunol 2004;22:563–598
7. Sasaki T, Irie-Sasaki J, Jones RG, et al. Function of PI3Kgamma in thymocyte development, T cell activation, and neutrophil migration. Science 2000;287:1040–1046
8. Camps M, Rückle T, Ji H, et al. Blockade of PI3Kgamma suppresses joint inflammation and damage in mouse models of rheumatoid arthritis. Nat Med 2005;11:936–943
9. Barber DF, Bartolomé A, Hernandez C, et al. PI3Kgamma inhibition blocks glomerulonephritis and extends lifespan in a mouse model of systemic lupus. Nat Med 2005;11:933–935
10. Thomas MJ, Smith A, Head DH, et al. Airway inflammation: chemokine-induced neutrophilia and the class I phosphoinositide 3-kinases. Eur J Immunol 2005;35:1283–1291
11. Filippi CM, von Herrath MG. Viral trigger for type 1 diabetes: pros and cons. Diabetes 2008;57:2863–2871
12. Mayer-Davis EJ, Bell RA, Dabelea D, et al.; SEARCH for Diabetes in Youth Study Group. The many faces of diabetes in American youth: type 1 and type 2 diabetes in five race and ethnic populations: the SEARCH for Diabetes in Youth Study. Diabetes Care 2009;32(Suppl. 2):S99–S101
13. Rewers M, Gottlieb P. Immunotherapy for the prevention and treatment of type 1 diabetes: human trials and a look into the future. Diabetes Care 2009;32:1769–1782
14. Anderson MS, Bluestone JA. The NOD mouse: a model of immune dysregulation. Annu Rev Immunol 2005;23:447–485
15. Trudeau JD, Kelly-Smith C, Verchere CB, et al. Prediction of spontaneous autoimmune diabetes in NOD mice by quantification of autoreactive T cells in peripheral blood. J Clin Invest 2003;111:217–223
16. Jin K, Song LF, He CM, Wang ZL, Hu XH, Wu XH. [Intervention effect of PI3Kgamma inhibitor AS605240 on autoimmune myocarditis in mice]. Sichuan Da Xue Xue Bao Yi Xue Ban 2009;40:817–820, 825
17. Wei X, Han J, Chen ZZ, et al. A phosphoinositide 3-kinase-gamma inhibitor, AS605240 prevents bleomycin-induced pulmonary fibrosis in rats. Biochem Biophys Res Commun 2010;397:311–317
18. Abdi R, Fiorina P, Adra CN, Atkinson M, Sayegh MH. Immunomodulation by mesenchymal stem cells: a potential therapeutic strategy for type 1 diabetes. Diabetes 2008;57:1759–1767
19. Fiorina P, Jurewicz M, Augello A, et al. Immunomodulatory function of bone marrow-derived mesenchymal stem cells in experimental autoimmune type 1 diabetes. J Immunol 2009;183:993–1004
20. Jurewicz M, Yang S, Augello A, et al. Congenic mesenchymal stem cell therapy reverses hyperglycemia in experimental type 1 diabetes. Diabetes 2010;59:3139–3147
21. Jindra PT, Hsueh A, Hong L, et al. Anti-MHC class I antibody activation of proliferation and survival signaling in murine cardiac allografts. J Immunol 2008;180:2214–2224
22. Bluestone JA, Herold K, Eisenbarth G. Genetics, pathogenesis and clinical interventions in type 1 diabetes. Nature 2010;464:1293–1300
23. Bassil R, Zhu B, Lahoud Y, et al. Notch ligand delta-like 4 blockade alleviates experimental autoimmune encephalomyelitis by promoting regulatory T cell development. J Immunol 2011;187:2322–2328
24. Gottschalk RA, Corse E, Allison JP. TCR ligand density and affinity determine peripheral induction of Foxp3 in vivo. J Exp Med 2010;207:1701–1711
25. Kim HP, Leonard WJ. CREB/ATF-dependent T cell receptor-induced FoxP3 gene expression: a role for DNA methylation. J Exp Med 2007;204:1543–1551
26. Best JL, Amezcua CA, Mayr B, et al. Identification of small-molecule antagonists that inhibit an activator: coactivator interaction. Proc Natl Acad Sci USA 2004;101:17622–17627
27. Matthews JB, Staeva TP, Bernstein PL, Peakman M, von Herrath M; ITN-JDRF Type 1 Diabetes Combination Therapy Assessment Group. Developing combination immunotherapies for type 1 diabetes: recommendations from the ITN-JDRF Type 1 Diabetes Combination Therapy Assessment Group. Clin Exp Immunol 2010;160:176–184
28. Bresson D, von Herrath M. Immunotherapy for the prevention and treatment of type 1 diabetes: optimizing the path from bench to bedside. Diabetes Care 2009;32:1753–1768
29. Luo X, Herold KC, Miller SD. Immunotherapy of type 1 diabetes: where are we and where should we be going? Immunity 2010;32:488–499
30. Fayard E, Moncayo G, Hemmings BA, Holländer GA. Phosphatidylinositol 3-kinase signaling in thymocytes: the need for stringent control. Sci Signal 2010;3:re5
31. Rodríguez-Borlado L, Barber DF, Hernández C, et al. Phosphatidylinositol 3-kinase regulates the CD4/CD8 T cell differentiation ratio. J Immunol 2003;170:4475–4482
32. Barber DF, Bartolomé A, Hernandez C, et al. Class IB-phosphatidylinositol 3-kinase (PI3K) deficiency ameliorates IA-PI3K-induced systemic lupus but not T cell invasion. J Immunol 2006;176:589–593
33. Barbi J, Cummings HE, Lu B, et al. PI3Kgamma (PI3Kgamma) is essential for efficient induction of CXCR3 on activated T cells. Blood 2008;112:3048–3051
34. Peng XD, Wu XH, Chen LJ, et al. Inhibition of phosphoinositide 3-kinase ameliorates dextran sodium sulfate-induced colitis in mice. J Pharmacol Exp Ther 2010;332:46–56
35. Schreiber A, Rolle S, Peripelittchenko L, et al. Phosphoinositol 3-kinase-gamma mediates antineutrophil cytoplasmic autoantibody-induced glomerulonephritis. Kidney Int 2010;77:118–128
36. Williams O, Houseman BT, Kunkel EJ, et al. Discovery of dual inhibitors of the immune cell PI3Ks p110delta and p110gamma: a prototype for new anti-inflammatory drugs. Chem Biol 2010;17:123–134
37. Tang Q, Bluestone JA. The Foxp3+ regulatory T cell: a jack of all trades, master of regulation. Nat Immunol 2008;9:239–244
38. Feuerer M, Shen Y, Littman DR, Benoist C, Mathis D. How punctual ablation of regulatory T cells unleashes an autoimmune lesion within the pancreatic islets. Immunity 2009;31:654–664
39. Atkinson MA, Wilson SB. Fatal attraction: chemokines and type 1 diabetes. J Clin Invest 2002;110:1611–1613
40. Emamaullee JA, Davis J, Merani S, et al. Inhibition of Th17 cells regulates autoimmune diabetes in NOD mice. Diabetes 2009;58:1302–1311
41. Rabinovitch A, Suarez-Pinzon WL. Roles of cytokines in the pathogenesis and therapy of type 1 diabetes. Cell Biochem Biophys 2007;48:159–163
42. Franceschini D, Paroli M, Francavilla V, et al. PD-L1 negatively regulates CD4+CD25+Foxp3+ Tregs by limiting STAT-5 phosphorylation in patients chronically infected with HCV. J Clin Invest 2009;119:551–564
43. Huber S, Schrader J, Fritz G, et al. P38 MAP kinase signaling is required for the conversion of CD4+CD25- T cells into iTreg. PLoS ONE 2008;3:e3302
44. Lee SM, Gao B, Fang D. FoxP3 maintains Treg unresponsiveness by selectively inhibiting the promoter DNA-binding activity of AP-1. Blood 2008; 111:3599–3606
45. Li L, Godfrey WR, Porter SB, et al. CD4+CD25+ regulatory T-cell lines from human cord blood have functional and molecular properties of T-cell anergy. Blood 2005;106:3068–3073
46. Ma J, Meng Y, Kwiatkowski DJ, et al. Mammalian target of rapamycin regulates murine and human cell differentiation through STAT3/p63/Jagged/Notch cascade. J Clin Invest 2010;120:103–114
47. Pallandre JR, Brillard E, Créhange G, et al. Role of STAT3 in CD4+CD25+FOXP3+ regulatory lymphocyte generation: implications in graft-versus-host disease and antitumor immunity. J Immunol 2007;179:7593–7604
48. Sauer S, Bruno L, Hertweck A, et al. T cell receptor signaling controls Foxp3 expression via PI3K, Akt, and mTOR. Proc Natl Acad Sci USA 2008; 105:7797–7802
49. Haxhinasto S, Mathis D, Benoist C. The AKT-mTOR axis regulates de novo differentiation of CD4+Foxp3+ cells. J Exp Med 2008;205:565–574
50. Chen G, Han G, Wang J, et al. Essential roles of TGF-beta in anti-CD3 antibody therapy: reversal of diabetes in nonobese diabetic mice independent of Foxp3+CD4+ regulatory T cells. J Leukoc Biol 2008;83:280–287
51. Valle A, Jofra T, Stabilini A, Atkinson M, Roncarolo MG, Battaglia M. Rapamycin prevents and breaks the anti-CD3-induced tolerance in NOD mice. Diabetes 2009;58:875–881
52. Keymeulen B, Vandemeulebroucke E, Ziegler AG, et al. Insulin needs after CD3-antibody therapy in new-onset type 1 diabetes. N Engl J Med 2005; 352:2598–2608
53. Baeder WL, Sredy J, Sehgal SN, Chang JY, Adams LM. Rapamycin prevents the onset of insulin-dependent diabetes mellitus (IDDM) in NOD mice. Clin Exp Immunol 1992;89:174–178